Civil Engineering Infrastructures Journal, 53(1): 71 – 88, June 2020
Print ISSN: 2322-2093; Online ISSN: 2423-6691
DOI: 10.22059/ceij.2020.271142.1531

Assessment of Near-Fault Ground Motion Effects on the Fragility Curves of Tall Steel Moment Resisting Frames

Mobinipour, S.A.[1] and Pourzeynali, S.[2*]

[1] Ph.D. Student, Department of Civil Engineering, Faculty of Engineering, University of Guilan, Rasht, Iran.
[2] Professor, Department of Civil Engineering, Faculty of Engineering, University of Guilan, Rasht, Iran.

Received: 09 Dec. 2018; Revised: 05 Mar. 2020; Accepted: 21 Apr. 2020

ABSTRACT: Nowadays it is common to use the fragility curves in probabilistic methods to determine the collapse probability resulting from an earthquake. The uncertainties exist in intensity and frequency content of the earthquake records are considered as the most effective parameters in developing the fragility curves. The pulse-type records reported in the near-fault regions might lead to the major damages in the structures having moderate and long periods since response spectra of near-fault ground motions within the long period range are different from those of the far-fault ground motions. In the present study, the influence of this type of earthquake records on the fragility curves of the steel special moment resisting frames, SMRFs, was examined. The results indicated that the median value of the collapse capacity (i.e. $\hat{S}_{Ct}$ Parameter, which defines the earthquake intensity leading to the collapse of the structure in half-set of the chosen records) due to near-fault ground motions was 76% that of the far-fault records for the ten-story example SMRF.

Keywords: Collapse Capacity, Collapse Damage Level, Fragility Curve, Near-Fault Ground Motions, Special Moment Resisting Frame (SMRF), Uncertainty.

INTRODUCTION

Preventing the collapse of structures is the main concern of modern guidelines aiming to assess structural performance against earthquake (FEMA, 2000a; ATC, 2011; UBC, 1997). Nowadays, one of the ways to assess the structural performance is use of the fragility curves (Krishna, 2017). These curves identify the probability of exceeding the structural damage from a certain level for the records imposed to the structure (Abdollahzadeh et al., 2015).

Fragility curves describe the dependency between earthquake intensity and seismic damage level. In order to precisely determine such a dependency, it is important to choose the earthquake intensity in the site at which the structure under the study is located (Pitilakis, 2015). Among the indicators representing the earthquake intensity, one might refer to the peak ground displacement (PGD), peak ground velocity (PGV), peak ground acceleration (PGA), and spectral acceleration in the period of the first mode of the structural vibration by taking into account 5% damping ratio $S_a(T_1,5\%)$ (Perrault and Gueguen, 2015). These curves are obtained

* Corresponding author E-mail: pourzeynali@guilan.ac.ir

through conducting logical regression analyses of the real or simulated damage data or numerical methods. As it was mentioned in the method of assessing the structural performance in guideline FEMA P-695 (FEMA, 2009), the current study used the spectral acceleration in the first-mode period of the structural vibration and 5% damping ratio $S_a(T_1,5\%)$ as the intensity measure of the earthquake.

Fragility curves are quite useful before and after the earthquakes. In addition to assessing the seismic risk, they are used to determine the priorities for rehabilitation of the structures, and management planning of the states and insurance companies which are responsible for estimating the extent of damage after the earthquake (Ruiz-García et al., 2010). On the other hand, considering the significance of near-fault ground motions and locating most of the metropolitans, e.g. Tehran and Tabriz in Iran, Los Angeles and San Francisco in USA, Osaka and Tokyo in Japan etc. near the active faults, seismic assessment of the structural performance is inevitable.

Although near-fault effects had been identified in the past, they were not well considered in the design of civil engineering structures until destructive earthquakes such as Landers in 1992, Northridge in 1994, Kobe in Japan in 1995, and Chi-Chi in Taiwan in 1999 (Choi et al., 2005; Galal and Ghobarah, 2006). During these earthquakes significant ground motion data were recorded near the causative faults which had pulse-type ground velocity records with long-pulse period with one or more peak points.

The velocity pulse in near-fault ground motions, resulting from the effects of progressive directivity, led to a sudden imposition of a large proportion of the earthquake energy to the structure in one or two pulses. In near-fault regions, the horizontal component of the acceleration record perpendicular to the fault has the highest effect on the response of structures and the effect of this component dominates that of the parallel to the fault component.

Moreover, if the vertical component is also important to the efficiency of the structure, the vertical vibration in near-fault regions should also be estimated (Bozorgnia and Bertero, 2004). It is noted that the present study does not consider the effect of this component. A large bulk of studies have shown that by increasing two parameters of the ratio of pulse period to the fundamental period of the structures, and the ratio of peak ground acceleration to the sideway stiffness of the structures, the non-linear response and structural damages increase in near-fault regions (Bai et al., 2019). Moreover, the concentration of the deformations in the lower part of the structures and increasing the axial force of the columns intensifies the effect of P-Δ in lower stories of the structure (Shehu et al., 2019).

Numerous studies have demonstrated that the distribution of the maximum stories ductility demand varies in the height of the structure depending on the characteristics of near-fault ground motions and vibrational characteristics of the structures (Sehhati et al., 2011). Some other studies have also shown that the distribution of the deformations of the structures depends on the ratio of structural period to the velocity pulse period in near-fault regions (Alavi and Krawinkler, 2001; Özhendekci and Özhendekci, 2012; Sehhati et al., 2011; Soleimani Amiri et al., 2013).

In dynamic analysis of structures subjected to lateral earthquake forces, motions with long-period pulses may have two different dynamic responses in the structure: first, the effect of forward-directivity, and second, the effect of permanent movement or fling-step (Vaez et al., 2013). Further observations indicate that, in the near-fault regions, considering the

permanent movement of the fling step effect parallel to the fault in Strike-slip fault types would lead to exciting the structures in the first mode, and vibrations due to pulse-type records without the fling-step effect would excite the higher modes of the structures (Kalkan and Kunnath, 2006).

Significance and effects of such records led to the current study to represent and develop the seismic fragility curves of steel moment frames for near-fault and far-fault ground motions. In this study, the building frames were modeled two-dimensionally by considering the nonlinear behavior of the structural members and utilizing the Opensees software. Having chosen near-fault and far-fault ground motions, over 1200 sets of non-linear time history analyses were conducted in the form of incremental dynamic analysis (IDA). The frames roof relative displacements (Roof drifts) were considered as the indicator of damage and capacities of the structures were determined through IDA, and the fragility curves were formed assuming the log-normal probability distribution.

FRAGILITY CURVES

In order to quantify the vulnerability of any structural/non-structural component, the probability of exceedance of a specific damage level can be defined in terms of an earthquake intensity measure, IM, e.g. PGD, PGV, PGA, or spectral acceleration response in the first-mode period of the structural vibration and 5% damping ratio $S_a(T_1,5\%)$, based on the extent of the earthquake risk. Repeating this operation for different IM values would form normalized curves called fragility curves. A fragility curve is generally defined as follows (Ji et al., 2007):

$$P_f = P[EDP_d \geq EDP_c|IM] \quad (1)$$

in which, EDP_d: is the engineering demand parameter; EDP_c: is the accepted value in the limit state; and IM: is the intensity measure. In the performance evaluation methodology of FEMA P-695, $S_a(T_1,5\%)$ is used as the intensity measure, IM parameter, and the current study also used the same indicator. Hence, the spectral acceleration response spectra with 5% damping ratio were calculated for all the records and used in the process of obtaining the fragility curves.

EDP_d is a value resulting from the non-linear incremental dynamic analysis (IDA), e.g. base shear, joint rotation, maximum story ductility demand, maximum roof deflection, maximum inter-story drift ratio θ_{max}. The criterion for choosing the type of this value results from the purpose of the study, for instance, the maximum story acceleration is used for non-structural damage while the maximum inter-story drift ratio θ_{max} is used for collapse. EDP_c in Eq. (1) is the acceptable value of the selected EDP_d quantity in the related limit state.

The analytical fragility curves are obtained based on analyzing various structural models designed according to the seismic guidelines and excited by the incremental intensities of the earthquakes. By increasing in the number of analyses, the level of error would decrease and results in curves with higher level of certainty. These analyses could be either non-linear time history analysis or non-linear static push-over analysis. When no adequate information about the real damage is available for the model under the study and the related earthquake data, then analytical fragility curves are being used to assess the structural performance. In this case, the analytical fragility curves are obtained through numerical simulation or random analysis of the structures exposed to the artificial records. It is commonly recommended to calibrate the obtained curves resulted from this method by means of

the results of real earthquakes. Allocating the simplified response models is an appropriate model for considering a larger number of structures since using analytical methods is limited due to time-consuming computational procedure.

In order to calculate the probability of exceedance, presented based on comparing the demand and capacity, Eq. (1), incremental dynamic analysis (IDA) is used which comprehensively discussed by Vamvatsikos and Cornell (2004). The procedure to develop the fragility curves through the incremental dynamic analysis (IDA) is summarized in the following steps (Marano et al., 2011; Zareian and Krawinkler, 2007):
a) Selecting the structural model with designed members; b) Defining the non-linear dynamic behavior (hysteresis behavior) of the structural members; c) Choosing a set of seismic acceleration records; d) Conducting incremental dynamic analyses (IDA); and e) Calculating the function parameters defining a fragility curve.

Uncertainties on Fragility Curves

Uncertainty in calculating EDP_d and/or EDP_c is due to the random nature of the seismic excitations known as aleatory uncertainty or record-to-record uncertainty and its influence is assessed in the form of a log-normal distribution with the mean value of 1 and standard deviation of β_{RTR} in the fragility curves. By taking into account the previously conducted studies by Ibarra et al. (2005) and Zareian et al. (2007), it might be concluded that the amount of uncertainty related to the selected records (β_{RTR}) is about 0.35-0.45 for various structural systems. These studies have demonstrated that considering a record-to-record uncertainty equal to β_{RTR}= 0.4 would lead to acceptable assessment of the structural performance (FEMA, 2000b). Hence, FEMA P-695 confines the amount of uncertainty related to the set of earthquake acceleration records to about 0.4 and presents the following equation for its relationship with the structural ductility μ_T (FEMA, 2009):

$$\beta_{RTR} = 0.1 + 0.1\,\mu T \leq 0.4 \qquad (2)$$

In the present study the uncertainty related to the selected earthquake acceleration records is assumed as β_{RTR} = 0.4.

Nevertheless, lack of adequate knowledge of the "real model of structures" results in uncertainty called epistemic uncertainty. Accordingly, FEMA P-695 (FEMA, 2009) categorizes the influential factors on this uncertainty and presents log-normal standard deviation corresponding to various conditions of each case. These factors are as follows:

Uncertainty in modeling (β_{MDL}) is related to the fact that in what extent the structural model(s) are able to consider the structural response and influential parameters on the design space of the given structural class. In addition, it is related to the degree of effectiveness and precision of the analytical models used in simulating the behavior of the structure and its members at the collapse threshold level.

Table 5-3 given in FEMA P-695 (FEMA, 2009), displays the qualitative ranking of the design models and presents the related amount of uncertainties to take into account the completeness of the selected non-linear model of structural behavior in covering the simplified assumptions made in the design, and its ability in considering all structural collapse modes. In the present study, the ability of the structural model in representing the collapse characteristics is considered to be medium; and accuracy and robustness of the models are also assumed to be medium, and therefore, by referring to the above table the value of β_{MDL} is taken about 0.35.

Uncertainty resulting from the design requirements (β_{DR}) is related to the

reliability of the design requirements to avoid the collapse of the structure in the unpredicted damage modes. For instance, the requirements of the currently valid guidelines for the steel and reinforced concrete special moment frames were based on the precise experimental results and their performance is assessed in seismic events.

Moreover, the requirements of their design entail capacity-based design which provides adequate safety to avoid unpredicted behaviors. Hence, if the requirements to design these models are qualitatively assessed as Excellent then β_{DR} = 0.10 can be used. Table 3-1 of the FEMA P-695 instruction (FEMA, 2009) provides structural design uncertainty regarding the degree of completeness of design assumptions and available information on structural design**.** In the present study, the ability to adhere to design principles in quality rating of design requirements is considered to be medium and therefore, by referring to the above table the value of β_{DR} is taken about 0.35 (FEMA, 2009).

Uncertainty in experimental results (β_{TD}) corresponds to the comprehensiveness and precision of the used experimental information in defining the behavior of members of a structural system and depends on the extent of knowledge about the materials behavior, members, connections, and experiment devices. Although this uncertainty is closely associated with the uncertainty resulting from modeling, it is different in terms of the extent of precision. Table 3-2 given in FEMA P-695 shows the results of experiments. In the present study, the completeness of experimental information is considered to be low and confidence of test results is assumed to be poor, and therefore, by referring to the above table the value of β_{TD} is taken about 0.5 (FEMA, 2009).

Combining Sources of Uncertainties in Assessing the Collapse Performance of Structures

The fundamental issue which deserves attention in preparing the fragility curves is that a rational mathematical method is to be used to combine the existing statistical data. Various types of data are to be weighed in terms of precision when statistical analyses are being conducted. To this end, in order to gain collapse fragility curve for a given significant sample model, it is required the following two parameters to be determined:

- Median value of the spectral acceleration corresponding to the collapse level in the fundamental period of the structure $(\hat{S}_{CT})$.
- Total uncertainty which is effective in evaluating the performance of the structure under consideration (β_{Tot}).

Collapse intensity level for a specific structural model is defined through using a random variable called S_{CT}. This variable is obtained through multiplying median spectral acceleration corresponding to the collapse $(\hat{S}_{CT})$ level by a random variable λ_{Tot} (FEMA, 2009):

$$S_{CT} = \hat{\mathrm{S}}_{\mathrm{CT}}.\lambda_{\mathrm{Tot}} \tag{3}$$

in which λ_{Tot}: follows a log-normal distribution with the mean value of 1 and a standard deviation of β_{Tot} given as follows:

$$\lambda_{\mathrm{Tot}} = \lambda_{\mathrm{RTR}}.\lambda_{\mathrm{DR}}.\lambda_{\mathrm{TD}}.\lambda_{\mathrm{MDL}} \tag{4}$$

where λ_{RTR}, λ_{DR}, λ_{TD}, and λ_{MDL}: are independent parameters following log-normal distribution with a unit mean value and standard deviations of β_{RTR}, β_{DR}, β_{TD}, and β_{MDL}, respectively. Since these parameters are also assumed to be statistically independent, the total standard deviation in log-normal distribution related to Eq. (4) is calculated as follows:

$$\beta_{Tot} = \sqrt{(\beta_{\mathrm{RTR}}^2 + \beta_{\mathrm{DR}}^2 + \beta_{\mathrm{MDL}}^2 + \beta_{\mathrm{TD}}^2)} \qquad (5)$$

in which β_{Tot}: is the total uncertainty in assessing the structural collapse; and the other parameters are defined in previous sections. In the current study, by considering the uncertainty values explained earlier, the total uncertainty of Eq. (5) equals to 0.809.

Definition of Limit States to Prepare the Fragility Curves

The fragility curves express the probability of failure corresponding to a given state of failure at several levels of earthquake seismic movements. In fact, the fragility curve describes the ratio between the magnitude of the earthquake and the level of probable seismic failure. Different methods can be used to determine damage indices as functions of specific response parameters. The damage index can be expressed either for the whole structure or for a member. Indicators that indicate the magnitude of earthquakes suitable for fragility analysis can include maximum deformation, hysterical behavior and deformation and energy absorption of structures. Deformation based on non-cumulative damage indices as the drift ratio and the displacement ductility, have the advantage of simplicity in calculations (Marano et al., 2011).

For these reason, the inter-story drift index, will be used in the present study. To develop the fragility curves, it is necessary to calibrate the relationship between damage level and inter-story drift.

In the present study, the relationships between damage states and inter-story drift ratio provided by the Hazus®-MH MR5 (HAZUS-MH, 2011) database and FEMA-350 (FEMA, 2000c) are chosen.

From the incremental dynamic analysis (IDA), the damage parameters are obtained and damage of the structures is quantified based on the inter-story drift ratio of the structure for HAZUS and FEMA methodology.

In Hazus®-MH MR5 formulation, for high-rise steel building structures with moment resisting frame system, the damage levels are defined based on the inter-story drift ratio as follows:

a. Slight damage level: in this damage level, slight deformations are created in the structure and slight cracks might occur in few numbers of welded parts.

b. Moderate damage level: some of the structural members might reach yielding level and in some welded or bolted connections, crack or fracture may be observed.

c. Extensive damage level: in this case, most structural members surpass the yielding point which leads to permanent deformation of the structure. Some of the members and/or connections might surpass their ultimate capacity observed in the form of connections damage or extensive deformation.

d. Complete damage level: a considerable proportion of the structural elements surpass their ultimate bearing capacity which leads to hazardous lateral deformations or structure collapse threshold.

In HAZUS the inter-story relative displacement to the story height ratios (drift ratios) associated with slight damage state, moderate damage state, extensive damage state, and complete damage state are set to be 0.3%, 0.6%, 1.5%, and 4%, respectively, based on non-linear analysis.

In FEMA-350 formulation, two discrete structural performance levels, Immediate Occupancy (IO) and Collapse Prevention (CP), are defined.

a. Immediate Occupancy performance level (IO): The immediate occupancy structural performance level is defined as the building space and systems are anticipated to be fairly usable. However, equipment and

contents are generally secure but may not operate due to mechanical failure or lack of utilities. The structure experience light damages, but there are no permanent drifts. Steel moment frames experience minor local yielding in few locations. No buckling, fracture, and observable distortion of members. Lastly, braces of braced steel frame structure suffer minor yielding or distortion (FEMA, 2000c).

b. Collapse Prevention performance level (CP): The collapse prevention structural performance level is defined as the building damage is severe, the structure retains little residual stiffness and strength. The building suffers large permanent drifts. However, load bearing columns and walls function. Beams and columns distort heavily in steel frames and even many of them along with their connections could fail. Added to that, several moment connections fracture. Nonstructural components damage extensively (FEMA, 2000c).

FIMA-350 instructions provide values for global inter-story drift ratio capacity for regular, well-configured structures. According to this section of the guide for special moment resisting frames (SMRF), the immediate occupancy performance level (IO) corresponds to inter-story relative displacement to the story height ratios (drift ratios) of 2% and the collapse prevention performance level (CP) corresponds to the displacement in which the slope of the IDA curve reaches 20% of the initial elastic slope or the maximum story drift ratio reaches to about 10% (whichever happens first).

NUMERICAL STUDIES

In the present study, as shown in Figure 1, one typical symmetric building plan with two heights, one ten-story and the other one twenty-story, are chosen for the numerical study to assess the effect of near-fault ground motions on their fragility curves. Since the selected buildings in present study are symmetric and regular in both aspects of height and plan; therefore, for these buildings, a two-dimensional analysis is sufficient.

The first step in preparing the fragility curve is to determine the collapse capacity of the structures due to the earthquake records. In order to ensure access to adequate precision in capacity assessment of the structure, a large number of reported records in the next generation attenuation (NGA) database provided by the Pacific earthquake engineering research center (PEER) is utilized. A total number of 28 near-fault accelerogram records and 39 far-fault ones all with magnitude Mw equal and greater than 6.5 are chosen. Having chosen a quite large number of records, it was tried to calculate the intensity measure (IM) of collapse level of the structures.

IDA was used to assess the structural collapse level. Choosing a desired IM made it possible to cover all ranges of seismic responses from linear elastic to non-linear and collapse stages of the structures. In order to fulfill this goal, Hunt and Fill algorithm (Vamvatsikos and Cornell, 2004), was used and all the earthquake records were scaled from a small-scale coefficient (0.05g) to a scale coefficient corresponding to the collapse level for using in the IDA procedure. By choosing this algorithm and conducting more than 1200 non-linear dynamic analyses, the fragility curves were prepared at various levels of performance to investigate the effects of ground motion types.

Modeling and Design of Steel Special Moment Resisting Frames

The selected structures in the current study were two ten and twenty-story Steel Special Moment Resisting Frames (SMRF) with similar plan (See Figure 1). In these frames,

W14 and W16 cross sections were used for the columns and beams, respectively. Selection of these types of profiles is due to their high capacity of plastic rotation; appropriate and useful behavioral information (Lignos et al., 2011). The deterioration model presented by Ibara et al. (2005) was the basis of the dynamic non-linear hysteretic model used in his study. The modified model of Ibara-Winkler (Ibara et al., 2005) was based on a push curve and a set of regulations defining the inter-boundary hysteresis behavior properties.

In order to impose damping on the structures under the study, a Rayleigh-type damping modeling method was used based on the study by Zareian and Medina (2010) which considers the damping ratio of 5% for the first and fifth modes (since the first five modes were sufficient to include 95% of mass in computations).

Selected Earthquake Acceleration Records

One of the most important parts which has a direct influence on the results and seismic performance assessment of the structures in IDA is choosing the earthquake records. To this end, the selected acceleration records should meet the following requirements (FEMA, 2009):

a. Requirements of section 16.1.3 of the ASCE/SEI 7-10 (ASCE, 2010) guideline. Based on this section of the code, the ground motions shall be scaled such that the average value of the 5 percent damped response spectra is not less than the design response spectrum in the period range of 0.2T to 1.5T where T is the fundamental natural period of the structure in the direction of response under the study (ASCE/SEI 7-10, 2010).

b. Records should represent the high ground motions related to the maximum considered earthquake (MCE).

In FEMA P-695 performance assessment procedure, there are two sets of different records to assess the structural performance including far-fault and near-fault record sets.

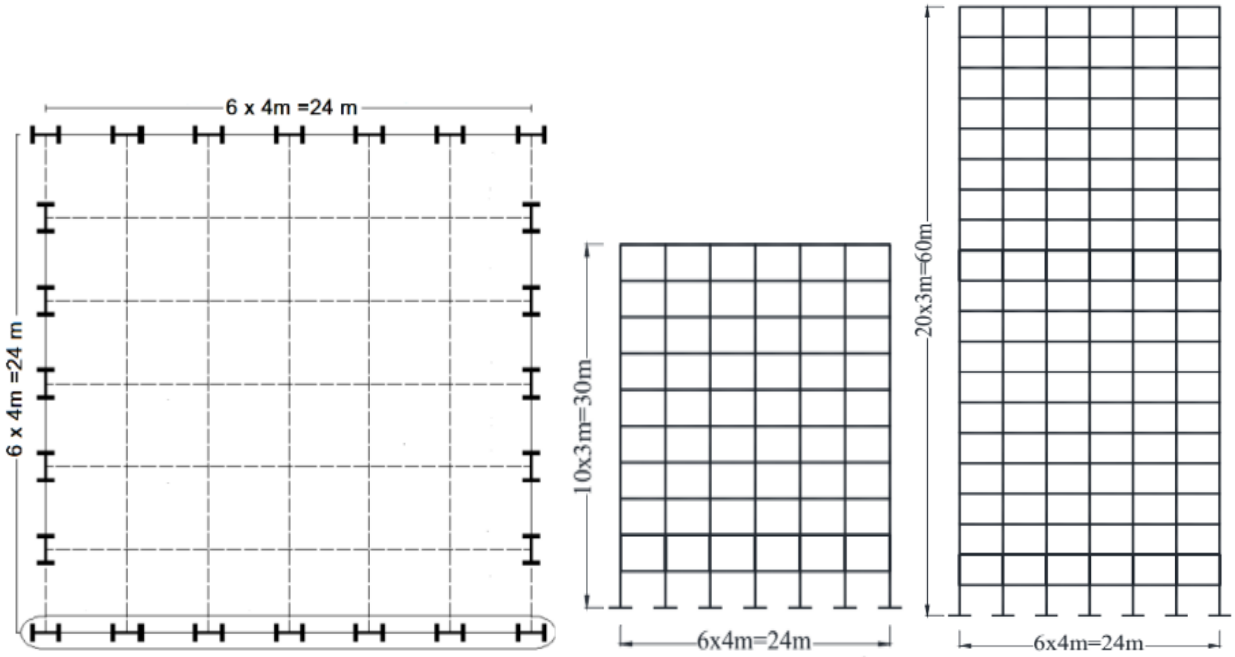

Fig. 1. a) The typical plan of the buildings used in this study, and b) Elevation of ten and twenty-story steel special moment frames

In the present study, the set of far-fault ground motions includes 39 components of horizontal acceleration records of the earthquakes which were recorded in a distance of greater than 10 km from the fault rupture location and having no velocity pulse.

The set of near-fault ground motions includes 28 components of horizontal acceleration records of the earthquakes which were recorded in a distance of less than 10 km from the fault rupture location and include the velocity pulse (FEMA, 2009).

A quite large number of the earthquake records are selected all from PEER database to provide adequate number of records to estimate the record-to-record uncertainty β_{RTR}, and make it possible to better evaluate the collapse median level of earthquake intensity. However, explicit and direct calculation of the record-to-record uncertainty parameter is not required in FEMA P-695 performance assessment procedure, since a large number of statistical studies on the set of selected records have shown that using a record-to-record uncertainty of β_{RTR} = 0.4 suffices to assess various structural systems performance level.

In spite of this, in the present study, in order to estimate this uncertainty more precisely, its value is calculated according to Eq. (2). All the selected records have PGA > 0.15g, and $M_w \geq 6.5$; and the peak ground acceleration (PGA) values of the near-fault ground motions range from 0.15g to 0.84g with a mean value of $\overline{PGA}$ = 0.50g. It is worth noting that if the selected sets of records cover all existing dispersion factors, a more precise estimation of the structural behavior would be possible (FEMA, 2009).

The most important characteristics of each far-fault and near-fault sets of earthquake acceleration records are provided in Tables A1 and A2, respectively, given in Appendix.

Results of IDA Fragility Curves at the Performance Levels of the Structures

Having conducted non-linear Incremental Dynamic Analysis (IDA) for the selected frames, the corresponding collapse fragility curves were prepared. The spectral acceleration of the record set at the specified period is S_T, and the intensity at the collapse point for each record is S_{CT}. The median collapse intensity for the entire record set (the median of 28 and 39 records to near-field and far- field sets respectively) is $\hat{S}_{Ct}$ (FEMA, 2009).

The figures provided in this section display the results of this procedure for the structural frames under the study. The findings presented in the figures, resulted from over 1200 non-linear incremental dynamic analyses conducted for each model for the scaled acceleration records ranging from 0.05 g to the corresponding performance level defined in the guidelines.

Figures 2 to 5 show the fragility curves of the example ten-story moment resisting frame under application of the near-fault and far-fault acceleration records. In Figure 2, the fragility curves resulted from IDA are compared for the performance levels given in HAZUS guideline.

Figure 3 also displays the same IDA results for the performance levels given in FEMA-350 (IO and CP levels). The points in Figure 3 display the results of the IDA analysis of the structures under the influence of 28 near-field record and 39 far-field records in both IO and CP performance level (i.e., there is a point for each particular record that indicates the exceeding probability of damage of the structure from the IO or CP level under that particular record). While the lines show this probability of exceedance, if the log-normal distribution is assumed. As these figures display, the slope of the fragility curves in both cases, (Gerami and Abdollahzadeh, 2015) under the influence of

near and far fault records, decreases from the slight damage state to the complete damage state, i.e. the efficiency of the structure at the time of complete damage are higher than that of the other damage states for a given IM level. This might result from the structural ductility, i.e. at the state of complete damage the structure enters to a non-linear state and shows a flexible behavior.

Figure 4 compares the fragility curves of the ten-story steel moment frame due to near-fault and far-fault ground motions, according the HAZUS guideline. These curves display that the response of the frame under near fault records is much critical than those of the far fault records. Increasing seismic demands in structures under the influence of near-field records can be attributed to the presence of pulse velocities in near-fault ground motions.

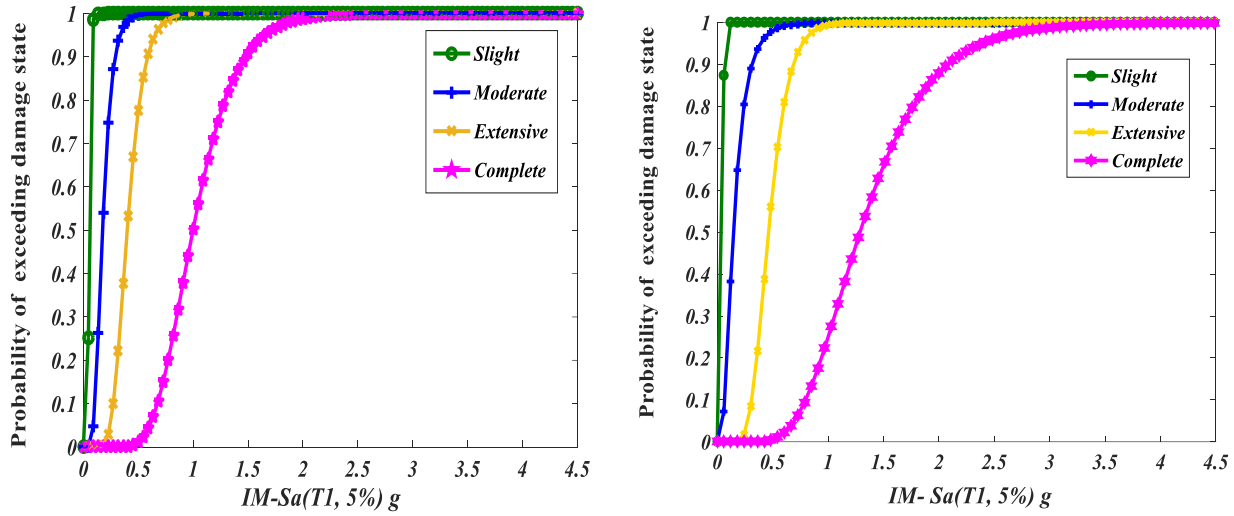

(a) (b)

Fig. 2. Damage Fragility curves using HAZUS limit states for the ten-story steel moment frame under: a) near-fault ground motions; and b) far-fault ground motions

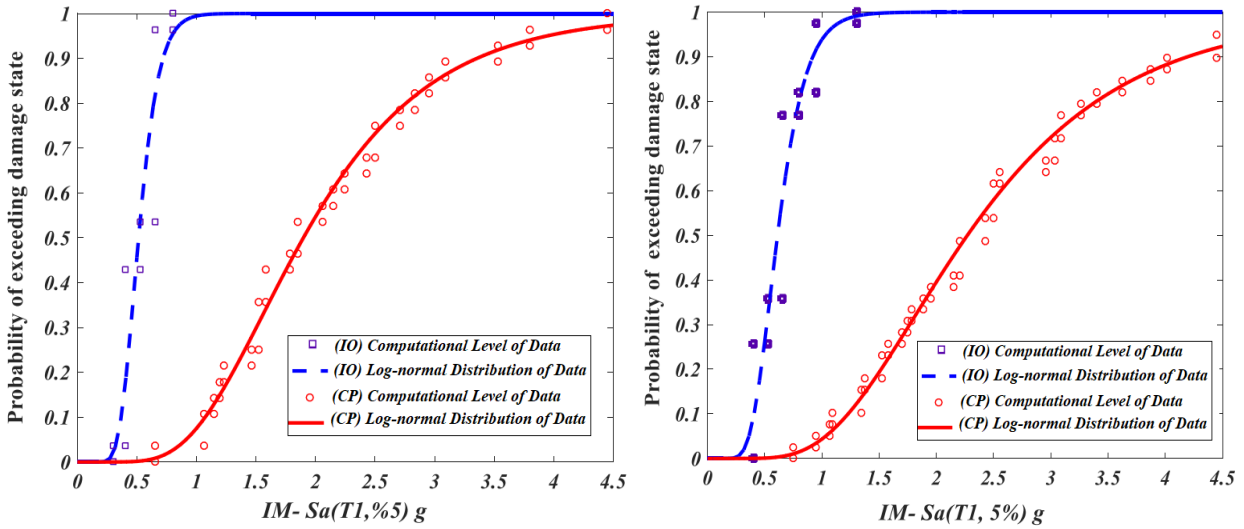

(a) (b)

Fig. 3. Damage Fragility curves using FEMA-350 limit states for the ten-story steel moment frame under: a) near-fault ground motions; and b) far-fault ground motions

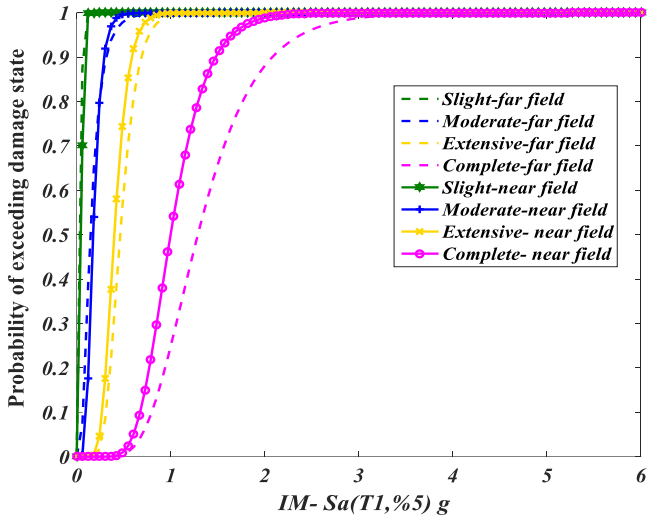

Fig. 4. Comparison of the fragility curves of the ten-story steel moment frame due to near-fault and far-fault ground motions, according the HAZUS

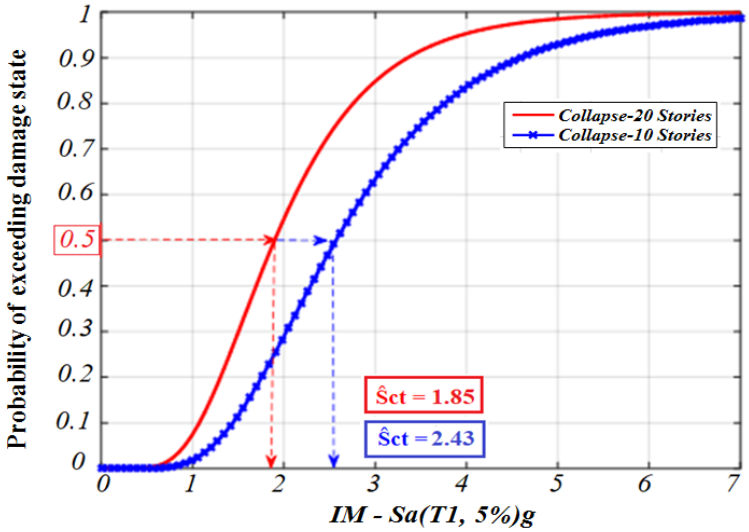

Fig. 5. Median values of the ten-story steel moment frame at collapse level under: Near fault ground motions $\hat{S}_{Ct}$ = 1.85 and far fault ground motions $\hat{S}_{Ct}$ = 2.43, according FEMA P-695

Figure 5 compares the collapse capacity median values ($\hat{S}_{Ct}$) of the IM levels of the ten-story frame under the application of both near and far-fault ground motions based on the FEMA-350 (FEMA, 2000c) definition. As it can be seen from the figure, the collapse capacity median value ($\hat{S}_{Ct}$), which defines the earthquake intensity measure that leads to the collapse of the structure in half of the earthquakes, for near-fault ground motions is about 76% that of the far fault records. This reduction trend in the collapse capacity of the frames might result from the velocity pulses exist in the near-fault ground motions due to the forward directivity effects. The presence of such pulses causes that a large proportion of the earthquake energy to be suddenly imposed in one or two pulses to the structure, and thereby, makes the most impact on the deformation demand in the structural responses.

Research studies show that distribution of the maximum story ductility demands varies within the height of the structures depending

on the characteristics of the near-fault ground motions and the vibrational properties of the structures such that in some cases the lower part of the structure is critical while in some others, the mid parts are critical. Some studies have argued that the distribution of the structural ductility within the height would depend on the ratio of the structure's vibration period to the velocity pulse period in near-fault ground motions (Alavi and Krawinkler, 2001; Sehhati et al., 2011). Investigations have shown that seismic behavior of the structures would be stiff or soft in near-fault regions due to forward directivity effects (Gerami and Abdollahzadeh, 2015).

Figures 6 to 9 display the fragility curves for the example twenty-story moment resisting frame. There is a significant difference between the results of this frame with those of the ten-story frame. This difference is notable on the value of collapse capacity median ($\hat{S}_{Ct}$) corresponding to near fault and far fault records.

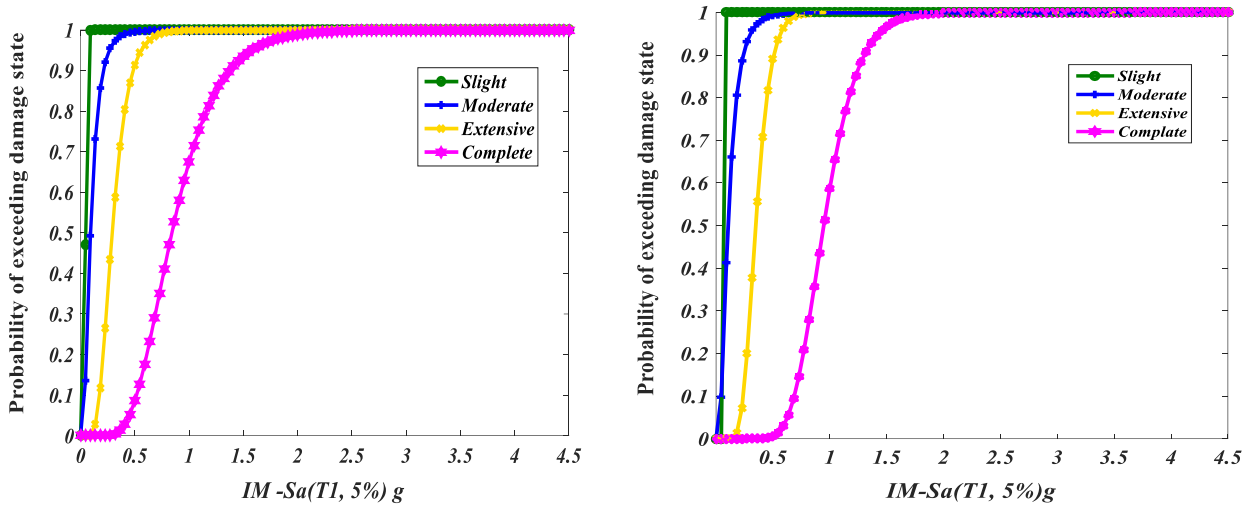

(a) (b)

Fig. 6. Damage Fragility curves using HAZUS limit states for the twenty -story steel moment frame under: a) near-fault ground motions; and b) far-fault ground motions

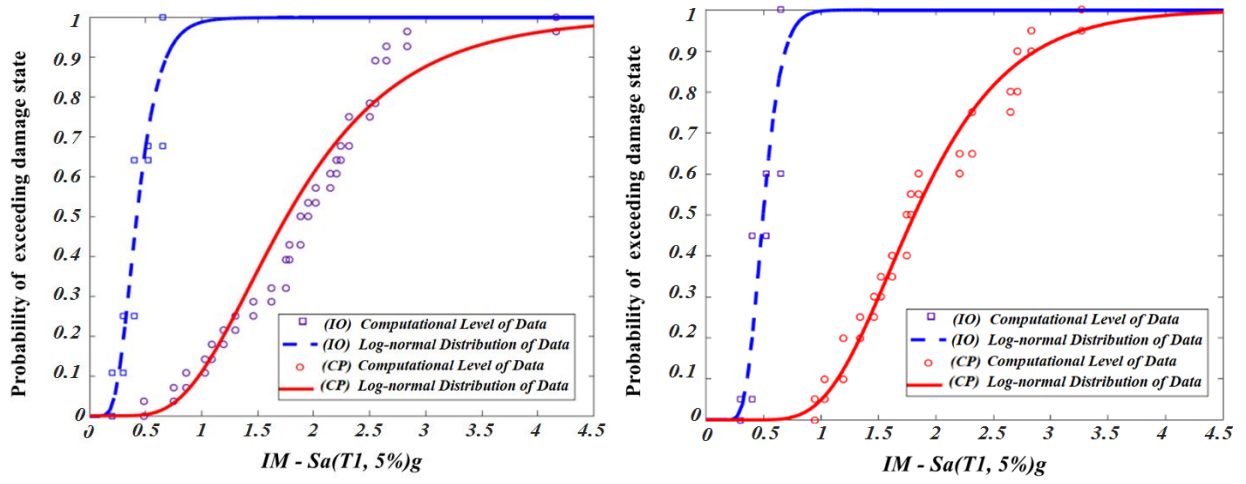

(a) (b)

Fig. 7. Damage Fragility curves using FEMA-350 limit states for the twenty -story steel moment frame under: a) near-fault; and b) far-fault ground motions

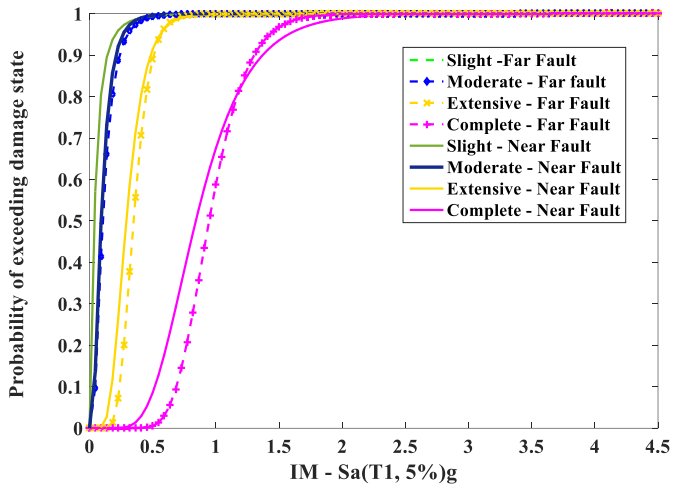

Fig. 8. Comparison of the fragility curves of the twenty-story steel moment frame due to near-fault and far-fault ground motions (according to HAZUS)

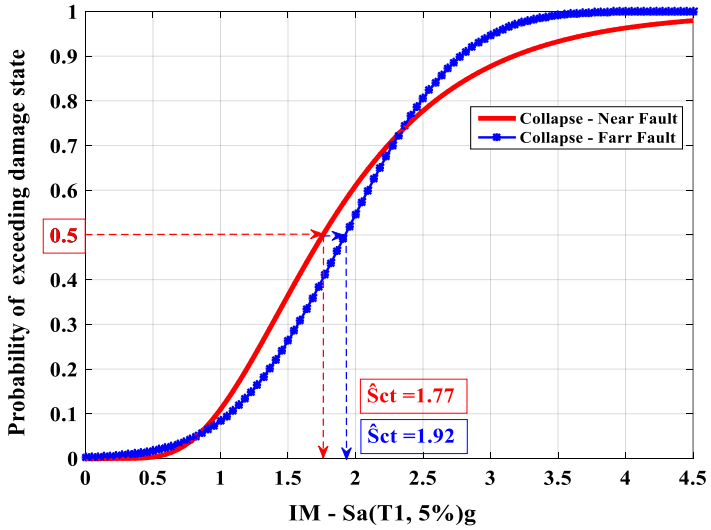

Fig. 9. Median values of the twenty-story steel moment frame at collapse level under: near-fault ground motions $\hat{S}_{Ct}$ = 1.77 and far-fault ground motions $\hat{S}_{Ct}$ = 1.92

In this structure, the collapse capacity median value due to near fault records was about 92% of that due to far fault ones (compared to 76% with the ten-story structure). This might indicate that an increase in the number of stories in tall structures would increase the influence of far fault earthquakes on the structure seismic response so that no significant difference is observed between the structure seismic demand due to near-fault and far-fault records.

Figure 10 compares the fragility curves of example ten-story and twenty-story steel moment frames. As it can be seen from the figure, differences between the fragility curves and the IM median values at collapse performance level in the example ten-story and twenty-story frames are more under far-fault ground motions compared to those of the near-fault ground motions. This confirms that the seismic demand increasing rate in tall building structures with increasing the number of stories is higher in far-fault regions compared to that of the near-fault regions.

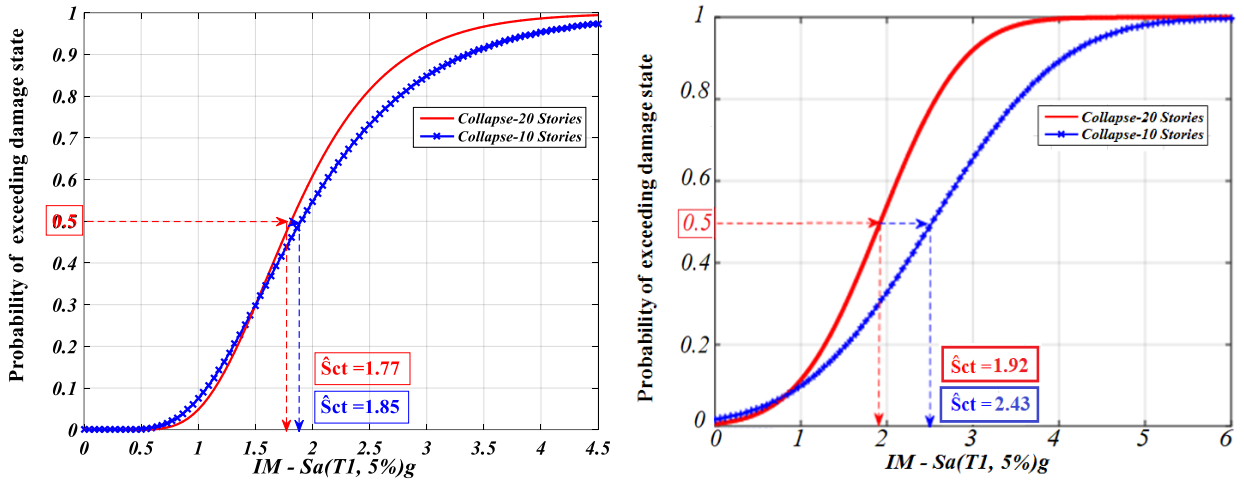

(a) (b)

Fig. 10. Comparison of the fragility curves of ten-story and twenty-story steel moment frames under: a) near-fault; and b) far-fault ground motions at collapse limit state (based on FEMA-350)

In the incremental dynamic analysis (IDA) method, when the far-fault ground motions are highly scaled up to represent extremely strong records, in fact they act as near-fault ground motions with high PGA values and several strong pulses. If displacement demand in the first strong pulse of the acceleration record causes the structure enters to non-linear region, then its stiffness decreases and vulnerability of the structure on tolerating subsequent damages caused by the rest of record would be increased. In near-fault ground motions, in which only one or two strong pulses exist at the beginning of the record, it seems less probable for the structure to be imposed by a displacement demand similar to the aforementioned pulses which compose the far-fault ground motions. In the present study, it was found that an increase in the structure demand with higher values of the acceleration index was higher in far-fault ground motions compared to near-fault ground motions (Figure 10).

CONCLUSIONS

In the present study, fragility curves of special moment resisting frames of the tall steel building structures were examined for far-fault and near-fault ground motions. The selected earthquake records included 28 near-fault and 39 far-fault ground motions reported in the Next Generation Attenuation (NGA) database related to the Pacific Earthquake Engineering Research Center (PEER). The quite large number of records is due to the fact that considering record-to-record uncertainty (β_{RTR}) requires an adequate number of records. Moreover, it would make it possible to evaluate the earthquake intensity of median collapse level more precisely. The structures under the study were modeled two-dimensionally by considering the nonlinear behavior of the structural members and utilizing the Opensees software.

The deterioration model given by Ibarra (2005) and completed by Ibarra-Krawinkler (2009) was used as the basis of the dynamic nonlinear behavior of the model. In this model, the hysteresis behavior including cyclic deterioration velocity in two loading directions, residual strength and influence of ultimate deformation when the strength reaches to zero were modeled. Moreover, in the present study, for modeling the damping

matrix, Zareian and Medina (2010) methodology was used by choosing the structural damping ratio of 5% for the first and fifth modes of vibration. Using the HAZUS MH-MR5 and FEMA-350 guidelines and their introduced damage levels for the structural steel moment frames with moderate and high number of stories and based on the story drift ratio, the fragility curves were prepared by choosing the spectral acceleration response at the first-mode period and 5% damping ratio, $Sa(T_1,5\%)$, as the intensity measure, IM. In this study, by taking the intensity measure incremental steps from 0.05g to the collapse occurrence and conducting over than 1200 time-consuming and bothersome incremental non-linear dynamic analyses (IDA), the following results were obtained:

1. In general, the seismic response of the structures due to near-fault ground motions is more critical compared to that of the far-fault ones. In the current study, it is observed that the median value of the collapse capacity (i.e. $\hat{S}_{Ct}$ parameter, which defines the earthquake intensity leading to the collapse of the structure in half-set of the chosen earthquake records) due to near-fault ground motions was 76% that of the far-fault ground motions for a ten-story moment frame.

2. With increase in the number of stories in high-rise building structures, the effect of far-fault ground motions on seismic response of the structure increases such that no significant difference would be observed in the structural ductility demands due to near-fault and far-fault ground motions. For the twenty-story structural steel moment frame under the study, the median value of collapse capacity due to near-fault ground motions was about 92% that of far-fault ground motions (compared to 76% for the ten-story frame). This confirmed that with increasing the number of stories in tall building structures, the increase rate of seismic demand in far-fault regions is higher than that of near-fault regions. It should be noted that, in the present study, only two heights of buildings were studied, therefore to strength this result more investigations are needed. On the other hand, in the present study the selected near-fault pulse-like ground motions are scaled based on guidelines, while some people doubt scaling of these records. Maybe scaling of the records also caused this result, in which by doing more investigations can be verified.

3. The slope of the fragility curves in all cases of near-fault and far-fault ground motions decreases significantly from the slight level of damage to the collapse level. For lower $Sa(T_1,5\%)$ values, the probability of exceeding a damage state is more than that of higher $Sa(T_1,5\%)$ values, i.e. the efficiency and performance of the structure before collapse state is higher than those of the other damage levels. This might result from the structure ductility, and the fact that the structure enters a non-linear step in collapse level and displays a more flexible behavior.

4. Depending on the seismic characteristics of the near-fault ground motions and vibrational properties of the structure, distribution of the maximum story ductility demand varies within the height of the structure such that in some cases, the lower parts of the structure and in some other cases, the mid parts of the structure would be critical. The results of the present study demonstrated that the maximum story ductility demand of the high-rise building frames (more than 10 stories) would occur in the one-third lower part of the building.

5. It is observed that the type of record could influence the fragility curves of the structures and the collapse probability of the frames varies with type of the records. Moreover, with changing the record type from far-fault to near-fault would increase the collapse probability of the frames.

REFERENCES

Abdollahzadeh, G., Sazjini, M. and Asghari, A. (2015). "Seismic fragility assessment of Special Truss Moment Frames (STMF) using the capacity spectrum method", *Civil Engineering Infrastructures Journal*, 48(1), 1-8.

Alavi, B. and Krawinkler, H. (2001). *Effects of near-fault ground motions on frame structures*, Stanford: John A. Blume Earthquake Engineering Center, 301.

ATC (Applied Technology Council), (2011), Seismic performance assessment of buildings, Volume 1: Methodology, ATC-58-1 75% Draft, Redwood City, California.

Bozorgnia, Y. and Bertero, V.V. (2004). *Earthquake engineering: From engineering seismology to performance-based engineering*, CRC press.

FEMA. (2000a). *Prestandard and commentary for the seismic rehabilitation of buildings* FEMA-356, Federal Emergency Management Agency Washington, D.C.

FEMA. (2000b). *Recommended seismic evaluation and upgrade criteria for existing welded Steel moment-frame buildings* FEMA-351, Federal Emergency Management Agency, Washington, D.C.

FEMA. (2000c). *Recommended seismic design criteria for new steel moment frame buildings* FEMA-350, Federal Emergency Management Agency Washington, D.C.

FEMA. (2009). *Quantification of building seismic performance factors*, FEMA P-695, Federal Emergency Management Agency, Washington, D.C.

Gerami, M. and Abdollahzadeh, D. (2015). "Vulnerability of steel moment-resisting frames under effects of forward directivity", *The Structural Design of Tall and Special Buildings*, 24(2), 97-122.

HAZUS-MH. (2011). *Multi-hazard loss estimation methodology: Earthquake model*, In Hazus. ®. – MH MR5, User Manual.

Ibarra, L.F., Medina, R.A., and Krawinkler, H. (2005). "Hysteretic models that incorporate strength and stiffness deterioration", *Earthquake Engineering and Structural Dynamics*, 34(12), 1489-1511.

Ji, J., Elnashai, A.S. and Kuchma, D.A. (2007). *Seismic fragility assessment for reinforced concrete high-rise buildings*, MAE Center CD Release 07-14.

Kalkan, E. and Kunnath, S.K. (2006). "Effects of fling step and forward directivity on seismic response of buildings", *Earthquake Spectra*, 22(2), 367-390.

Krishna, K.G. (2017). Fragility analysis, A tool to assess seismic performance of structural systems", *Materials Today: Proceedings*, 4(9), 10565-10569.

Lignos, D., Chung, Y., Nagae, T. and Nakashima, M. (2011). "Numerical and experimental evaluation of seismic capacity of high-rise steel buildings subjected to long duration earthquakes", *Computers and Str*uctures, 89(11-12), 959-967.

Marano, G.C., Greco, R. and Morrone, E. (2011). "Analytical evaluation of essential facilities fragility curves by using a stochastic approach", *Engineering Structures*, 33(1), 191-201.

Özhendekci, D. and Özhendekci, N. (2012). "Seismic performance of steel special moment resisting frames with different span arrangements", *Journal of Constructional Steel Researc*h, 72, 51-60.

Perrault, M. and Gueguen, P. (2015). "Correlation between ground motion and building response using California earthquake records", *Earthquake Spectra*, 31(4), 2027-2046.

Pitilakis, K. (2015). *Earthquake risk assessment: certitudes, fallacies, uncertainties and the quest for soundness perspectives on European earthquake engineering and seismology*, Springer, Cham, 59-95.

Ruiz-García, J., Gilmore, A.T. and Zuñiga-Cuevas, O. (2010). "Simplified DRIFT-BASED fragility assessment of confined Masonary buildings", *Proceedings of the 9th U.S. National and 10th Canadian Conference on Earthquake Engineering*, Canada, Toronto.

Sehhati, R., Rodriguez-Marek, A., ElGawady, M. and Cofer, W.F. (2011). "Effects of near-fault ground motions and equivalent pulses on multi-story structures", *Engineering Structures*, 33(3), 767-779.

Shehu, R., Angjeliu, G. and Bilgin, H. (2019). "A simple approach for the design of ductile earthquake-resisting frame structures counting for P-Delta effect", *Buildings*, 9(10), 216.

Soleimani Amiri, F., Ghodrati Amiri, G. and Razeghi, H. (2013). "Estimation of seismic demands of steel frames subjected to near-fault earthquakes having forward directivity and comparing with pushover analysis results", *The Structural Design of Tall and Special Buildings*, 22(13), 975-988.

UBC. (1997). *Uniform building code*, Whittier, CA.

Vamvatsikos, D. and Cornell, C.A. (2004). "Applied incremental dynamic analysis", *Earthquake Spectra*, 20(2), 523-553.

Zareian, F. and Krawinkler, H. (2007). "Assessment of probability of collapse and design for collapse safety", *Earthquake Engineering and Structural Dynamics*, 36(13), 1901-1914.

Zareian, F. and Medina, R.A. (2010). "A practical method for proper modeling of structural damping in inelastic *plane structural systems",* Computers and Structures, 88(1-2), 45-53.

Appendix: Near-Fault and Far-Fault Ground Motions Used in the Present Study

Table A1. Characteristics of the far-fault set of records used in the present study

NO.	NGA	Event	Year	Station name	M_w	Fault type	Duration[s]	PGA[g]
1	68	San_Fernando	1971	LA-Hollywood_Stor_FF	6.6	Reverse	27.99	0.21
2	68	San_Fernando	1971	LA-Hollywood_Stor_FF	6.6	Reverse	27.99	0.17
3	125	Friuli-Italy-01	1976	Tolmezzo	6.5	Reverse	36.34	0.35
4	125	Friuli-Italy-01	1976	Tolmezzo	6.5	Reverse	36.34	0.31
5	169	Imperial_Valley-06	1979	Delta	6.5	Strike-Slip	99.91	0.24
6	169	Imperial_Valley-06	1979	Delta	6.5	Strike-Slip	99.91	0.35
7	174	Imperial_Valley-06	1979	El_Centro_Array_#11	6.5	Strike-Slip	39.03	0.36
8	174	Imperial_Valley-06	1979	El_Centro_Array_#11	6.5	Strike-Slip	39.03	0.38
9	721	Superstition_Hills-02	1987	El_Centro_Imp._Co._Cent	6.5	Strike-Slip	39.995	0.36
10	721	Superstition_Hills-02	1987	El_Centro_Imp._Co._Cent	6.5	Strike-Slip	39.995	0.36
11	725	Superstition_Hills-02	1987	Poe_Road_(temp)	6.5	Strike-Slip	22.29	0.45
12	725	Superstition_Hills-02	1987	Poe_Road_(temp)	6.5	Strike-Slip	22.29	0.30
13	752	Loma_Prieta	1989	Capitola	6.9	Reverse-Oblique	39.95	0.53
14	752	Loma_Prieta	1989	Capitola	6.9	Reverse-Oblique	39.95	0.44
15	767	Loma_Prieta	1989	Gilroy_Array_#3	6.9	Reverse-Oblique	39.94	0.56
16	767	Loma_Prieta	1989	Gilroy_Array_#3	6.9	Reverse-Oblique	39.94	0.37
17	829	Cape_Mendocino	1992	Rio_Dell_Overpass-FF	7	Reverse	35.98	0.39
18	829	Cape_Mendocino	1992	Rio_Dell_Overpass-FF	7	Reverse	35.98	0.55
19	900	Landers	1992	Yermo_Fire_Station	7.3	Strike-Slip	43.98	0.24
20	900	Landers	1992	Yermo_Fire_Station	7.3	Strike-Slip	43.98	0.15
21	953	Northridge-01	1994	Beverly_Hills-14145_Mulhol	6.7	Reverse	29.98	0.42
22	953	Northridge-01	1994	Beverly_Hills-14145_Mulhol	6.7	Reverse	29.98	0.52
23	960	Northridge-01	1994	Canyon_Country-W_Lost_Cany	6.7	Reverse	19.98	0.41
24	960	Northridge-01	1994	Canyon_Country-W_Lost_Cany	6.7	Reverse	19.98	0.48
25	1111	Kobe-Japan	1995	Nishi-Akashi	6.9	Strike-Slip	40.95	0.51
26	1111	Kobe-Japan	1995	Nishi-Akashi	6.9	Strike-Slip	40.95	0.50
27	1116	Kobe-Japan	1995	Shin-Osaka	6.9	Strike-Slip	40.95	0.24
28	1116	Kobe-Japan	1995	Shin-Osaka	6.9	Strike-Slip	40.95	0.21
29	1148	Kocaeli-Turkey	1999	Arcelik	7.5	Strike-Slip	29.995	0.22
30	1148	Kocaeli-Turkey	1999	Arcelik	7.5	Strike-Slip	29.995	0.15
31	1158	Kocaeli-Turkey	1999	Duzce	7.5	Strike-Slip	27.18	0.31
32	1158	Kocaeli-Turkey	1999	Duzce	7.5	Strike-Slip	27.18	0.36
33	1244	Chi-Chi-Taiwan	1999	CHY101	7.6	Reverse-Oblique	89.995	0.35
34	1244	Chi-Chi-Taiwan	1999	CHY101	7.6	Reverse-Oblique	89.995	0.44
35	1602	Duzce-Turkey	1999	Bolu	7.1	Strike-Slip	55.89	0.73
36	1602	Duzce-Turkey	1999	Bolu	7.1	Strike-Slip	55.89	0.82
37	1787	Hector_Mine	1999	Hector	7.1	Strike-Slip	45.3	0.27
38	1787	Hector_Mine	1999	Hector	7.1	Strike-Slip	45.3	0.34
39	1787	Hector_Mine	1999	Hector	7.1	Strike-Slip	45.3	0.15

Table A2. Characteristics of the near-fault set of records used in the present study

NO.	NGA	Event	Year	Station name	M_w	Fault type	Tp [s]	PGV [cm/s]	PGA [g]	Duration [s]
1	181	Imperial_Valley-06	1979	El_Centro_Array_#6	6.5	Strike-Slip	2.70	111.9	0.41	39.03
2	181	Imperial_Valley-06	1979	El_Centro_Array_#6	6.5	Strike-Slip	3.84	121.6	0.44	39.03
3	182	Imperial_Valley-06	1979	El_Centro_Array_#7	6.5	Strike-Slip	4.47	108.8	0.34	36.815
4	182	Imperial_Valley-06	1979	El_Centro_Array_#7	6.5	Strike-Slip	4.17	111.9	0.46	36.815
5	292	Irpinia-Italy-01	1980	Sturno	6.9	Normal	3.27	41.5	0.25	39.3384
6	292	Irpinia-Italy-01	1980	Sturno	6.9	Normal	3.00	71.1	0.36	39.3384
7	723	Superstition_Hills-02	1987	Parachute_Test_Site	6.5	Strike-Slip	2.31	143.9	0.46	22.34
8	723	Superstition_Hills-02	1987	Parachute_Test_Site	6.5	Strike-Slip	2.39	106.8	0.38	22.3
9	802	Loma_Prieta	1989	Saratoga-Aloha_Ave	6.9	Reverse-Oblique	1.83	55.6	0.51	39.95
10	802	Loma_Prieta	1989	Saratoga-Aloha_Ave	6.9	Reverse-Oblique	4.52	53.5	0.32	39.95
11	821	Erzican-Turkey	1992	Erzincan	6.7	Strike-Slip	2.87	95.4	0.50	20.775
12	821	Erzican-Turkey	1992	Erzincan	6.7	Strike-Slip	2.57	95.4	0.52	21.305
13	828	Cape_Mendocino	1992	Petrolia	7	Reverse	3.00	82.1	0.59	35.98
14	828	Cape_Mendocino	1992	Petrolia	7	Reverse	3.00	96.7	0.66	35.98
15	879	Landers	1992	Lucerne	7.3	Strike-Slip	5.12	132.3	0.73	48.12
16	879	Landers	1992	Lucerne	7.3	Strike-Slip	5.12	140.3	0.79	48.12
17	1063	Northridge-01	1994	Rinaldi_Receiving_Sta	6.7	Reverse	1.48	167.2	0.83	19.9
18	1063	Northridge-01	1994	Rinaldi_Receiving_Sta	6.7	Reverse	1.25	149.1	0.49	19.9
19	1086	Northridge-01	1994	Sylmar-Olive_View	6.7	Reverse	2.94	122.7	0.60	39.98
20	1086	Northridge-01	1994	Sylmar-Olive_View	6.7	Reverse	2.13	130.6	0.84	39.98
21	1165	Kocaeli-Turkey	1999	Izmit	7.5	Strike-Slip	5.37	52.0	0.22	29.995
22	1165	Kocaeli-Turkey	1999	Izmit	7.5	Strike-Slip	5.37	38.1	0.15	29.995
23	1503	Chi-Chi-Taiwan	1999	TCU065	7.6	Reverse-Oblique	5.74	136.5	0.81	89.995
24	1503	Chi-Chi-Taiwan	1999	TCU065	7.6	Reverse-Oblique	5.74	127.7	0.60	89.995
25	1529	Chi-Chi-Taiwan	1999	TCU102	7.6	Reverse-Oblique	9.81	106.6	0.30	89.995
26	1529	Chi-Chi-Taiwan	1999	TCU102	7.6	Reverse-Oblique	3.94	104.8	0.17	89.995
27	1605	Duzce-Turkey	1999	Duzce	7.1	Strike-Slip	7.74	78.9	0.35	25.88
28	1605	Duzce-Turkey	1999	Duzce	7.1	Strike-Slip	6.25	78.9	0.54	25.88